Available online at www.sciencedirect.com

SCIENCE DIRECT®

Journal of Photochemistry and Photobiology A: Chemistry 167 (2004) 17–22

Journal of Photochemistry and Photobiology A:Chemistry

www.elsevier.com/locate/jphotochem

Micelle-mediated UV-photoactivation route for the evolution of Pd_{core}–Au_{shell} and Pd_{core}–Ag_{shell} bimetallics from photogenerated Pd nanoparticles

Madhuri Mandal, Subrata Kundu, Sujit Kumar Ghosh, Tarasankar Pal*

Department of Chemistry, Indian Institute of Technology, Kharagpur 721302, India

Received 14 January 2004; received in revised form 2 March 2004; accepted 2 April 2004

Abstract

UV-photoactivation of aqueous $PdCl_2$ evolves palladium nanoparticles with narrow size distribution (~5 nm) in TX-100 [poly(oxyethylene)isooctyl phenyl ether] micelles. Here, TX-100 molecules serve as a stabilizer as well as a reducing agent. The layered core–shell bimetallic palladium–gold and palladium–silver colloids in the size range 10–30 nm have been prepared through successive ion loading by seed-mediated method where Pd particles act as seeds. By varying the seed to gold or silver ion ratios, palladium seeds are successfully covered by gold or silver shells of various compositions of Pd:Au and Pd:Ag. Thus, core–shell nanoparticles of various sizes are generated having tunable thickness of the shells. Optical plasmon absorption bands, transmission electron micrographs (TEM) and energy dispersive X-ray (EDX) studies characterize the particles.

Keywords: Palladium; Gold; Silver; TX-100; Core–shell; Bimetallic; UV-photoactivation

1. Introduction

Since recent past, many studies have been carried out on the materials in the nanoregime (especially the nanoparticles of noble metals) due to the achievement of unusual physicochemical properties, which are different from their bulk states. Because of their extremely small size and large specific surface area, metal nanoparticles show unusual behavior compare to the bulk metals. These particles are found to have potential applications in optoelectronics [1,2], drug delivery [3], catalysis [4–6], magnetostatics [7,8], etc.

Now a days bimetallic colloids, in which two kinds of metals are assembled in one entity and have become an attractive target to the researchers because of interesting scientific and technological applications. These colloids have well-different catalytic, electronic and optical properties [9] distinct from those of the corresponding monometallic particles. The catalytic activity, selectivity in catalytic reactions, physical and chemical stability of the bimetallic nanoparticles differs widely from that of their components [10,11]. Not only catalytic properties but also the electronic structures of such nanoscopic materials can be tailored by the changes in their compositions and structures. Researchers are getting interest from monometallic to bimetallic particles because of the change in the surface plasmon band energy relative to the separate metals [12]. Two main types of bimetallic nanoparticles exist, alloyed and layered (core–shell) nanoparticles. Depending on the content of the shell especially when it comes to Au or Ag those might be exploited in fluorescence, surface enhanced Raman scattering, catalysis, etc. Bimetallic colloids can be prepared by simultaneous co-reduction of two kinds of metal ions with or without protective agent (usually polymer or surfactant) or by successive reduction of one metal over the nuclei of another. Several methods for the preparation of bimetallic nanoparticles have been reported so far; such as (i) alcohol reduction [13–15], (ii) citrate reduction [16], (iii) polyol reduction [17,18], (iv) sonochemical method [19], (v) photolytic reduction [20], (vi) laser ablation method [21,22], (vii) γ-radiolysis technique [23], (viii) wet chemical method [24], etc. Their stability and sizes are controlled by the addition of protective agents such as soluble polymers, surfactants, organic ligands, etc. The size, structure and composition distribution of the resultant particles are all affected by the preparation conditions. Recently, we have demonstrated a new methodology to fabricate Au_{core}–Ag_{shell}

---

* Corresponding author. Tel.: +91-3222-283320;
fax: +91-3222-255303.
E-mail address: tpal@chem.iitkgp.ernet.in (T. Pal).

1010-6030/$ – see front matter © 2004 Elsevier B.V. All rights reserved.
doi:10.1016/j.jphotochem.2004.04.002

nanoparticles of various sizes using UV-irradiation technique [25]. To extend this technique, other binary systems like Pd/Au and Pd/Ag were targeted. It is worthy to understand whether or not the formation of any composite particle shares a common transition process with the morphological transformation as observed in the Au_{core}–Ag_{shell} bimetallics. Because of high catalytic activity of Pd [26], bimetallic colloids of gold and silver in combination with Pd are eminent member in the family of catalysts [27,28]. In these systems, incorporation of a second metal permits large changes in the catalytic properties of the active metal component [10]. The combination of gold and palladium is one of the most popular examples of bimetallic particles because they are miscible at any ratio as can be seen in their phase diagram. So it is easy to prepare Au/Pd alloyed bimetallic rather the core–shell one. In case of Ag/Pd particles, alloyed particles are mostly reported. The alloyed Ag/Pd particles are prepared via chemical [29,30], photochemical [31] and radiolytic reductions [32]. Au/Pd bimetallic nanoparticles in various molar ratios are prepared in reverse micelles by the co-reduction of $HAuCl_4$ and H_2PdCl_4 with hydrazine [33]. The formation of Au/Pd bimetallic particles having a Pd-rich shell by the alcoholic reduction method is reported recently [34]. In other studies both chemically [35] and sonochemically Au/Pd bimetallic particles leading to a Au_{core}–Pd_{shell} structure are reported [36,37]. Regarding Au/Pd, in maximum cases, Au_{core}–Pd_{shell} particles are formed. In most of these systems, segregation occurs during the reduction so that the more noble metal constitutes the core and the less noble metal the shell of a bilayered cluster. Henglein [38] reported the reduction of aqueous solution of $PdCl_4^{2-}$ by hydrogen to obtain palladium seed particles in the presence of sodium citrate as stabilizer and then used radiolytic methods to prepare bimetallic Pd_{core}–Au_{shell} and trimetallic Pd_{core}–Au_{shell}–Ag_{shell} particles. This communication reports for the first time a photochemical approach (here, UV-irradiation technique) that offers a simple and powerful method to synthesize monodisperse Au/Pd and Ag/Pd nanocolloids in micelle leading to the formation of Pd_{core}–Au_{shell} and Pd_{core}–Ag_{shell} structures. In our seed-mediated method, we used photochemically generated preformed Pd(0) particles as seed onto which the added metal ions like Au(III) or Ag(I) were adsorbed and subsequently reduced. Thus, keeping the Pd(0) in the core we can tune the shell structures (here Au or Ag as shell) of the bimetallic particles just optimizing the synthetic conditions.

2. Materials and methods

2.1. Instruments

UV-photoactivation was carried out by a photoreactor fitted with germicidal lamps of wavelength 365 nm (Sankyo, Denki, Japan). The photoreactor can produce a variable luminous flux from 100 to 850 lux. UV-Vis plasmon absorption band was measured by Shimadzu UV-160 digital spectrophotometer taking the solution in 1 cm quartz cuvette. Quantification of Au(III) and Ag(I) were done using ICP (ARL, France, Model No. 3410) instrument. TEM and EDX studies were performed using Hitachi S-4300 transmission electron microscope. Now, 2 μL of solution was spotted on carbon coated Cu grid and solvent was evaporated in vacuum desiccator.

2.2. Reagents

All the reagents were of AR grade. $PdCl_2$ and $HAuCl_4$ were purchased from Johnson Matthey, Royston, Hestfordshire, UK. $AgNO_3$ was purchased from Merck, India. TX-100 was purchased from SRL, India. Double distilled water was used throughout the entire course of investigation.

2.3. Procedure

At first we prepared Pd(0) seed particles in a quartz cuvette taking the $PdCl_2$ (2.2×10^{-4} M) solution in TX-100 (10^{-2} M; CMC of TX-100 $= 2 \times 10^{-4}$ M) medium under UV-light of 850 lux. The solution became black with brownish tinge in 30 min. Next, two sets of solutions were prepared: one set was with $HAuCl_4$ and another set was with $AgNO_3$ solution, respectively, but both containing Pd (5.5×10^{-5} M) as seeds in TX-100 medium. Then the mixtures were irradiated for 30 min. Again, successively required volumes of $HAuCl_4$ or $AgNO_3$ were introduced for different amount of ion loading to the respective cuvettes and were allowed to stand for 30 min. After addition of $HAuCl_4$ and $AgNO_3$ aliquots each time the reaction mixtures were irradiated for 30 min. After irradiation the black solution turned to hazy pink for gold loading indicating the formation of the Pd/Au bimetallic leading to Pd_{core}–Au_{shell} structure and brown indicating the formation of Pd_{core}–Ag_{shell} structure. Plasmon absorption band of both these sols were also recorded.

3. Results and discussions

UV-photoactivation of $PdCl_2$ has been found to evolve Pd nanoparticles with narrow size distribution in aqueous TX-100 micelles. Here, TX-100 molecules act as a reducing agent and stabilizer. The reduction process has been found to occur by the surfactant molecules below and above its CMC. Spectroscopically it was noted that Pd(II) from aqueous solution was consumed during photoreduction and the second observation was the consequence of the continuous absorption arose from interband transitions of the newly formed Pd colloids [39]. Exploiting the photoproduced Pd particles, i.e. seed particles, Pd_{core}–Au_{shell} or Pd_{core}–Ag_{shell} particles were produced again in TX-100 medium, via UV-photoactivation technique. The shells of Au and Ag resulted onto the Pd sur-

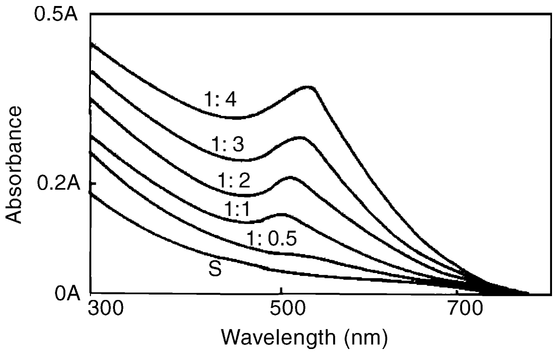

Fig. 1. Plasmon absorption spectrum of Pd(0) particles (S) and Pd_{core}–Au_{shell} of different composition. The molar ratio is given on the curves. Initial Pd(0) concentration is 5.5×10^{-5} M, [TX-100] = 10^{-2} M.

faces by the photoreduction of the added gold or silver ions those remained adsorbed onto the seeds. The optical spectra, TEM micrographs and EDX of the core–shell particles were recorded and compared with the published results.

It is to be mentioned that Au and Ag nanoparticles could be evolved even in the absence of Pd seed particles [40,41]. But this would be an uncatalysed evolution of particles. In the presence of preformed seed particles, surface catalysed growth of shell was observed. Again, the evolution of new nucleation centers become redundant under the experimental condition as the UV-source serves as a weak reducing agent [42].

Fig. 1 (curve S) shows the absorption spectrum of completely reduced Pd(0) sol in 10^{-2} M TX-100 medium. The solution had a black color with a brownish tinge. We used this solution as seeds (S) to prepare Pd_{core}–Au_{shell} and Pd_{core}–Ag_{shell} particles.

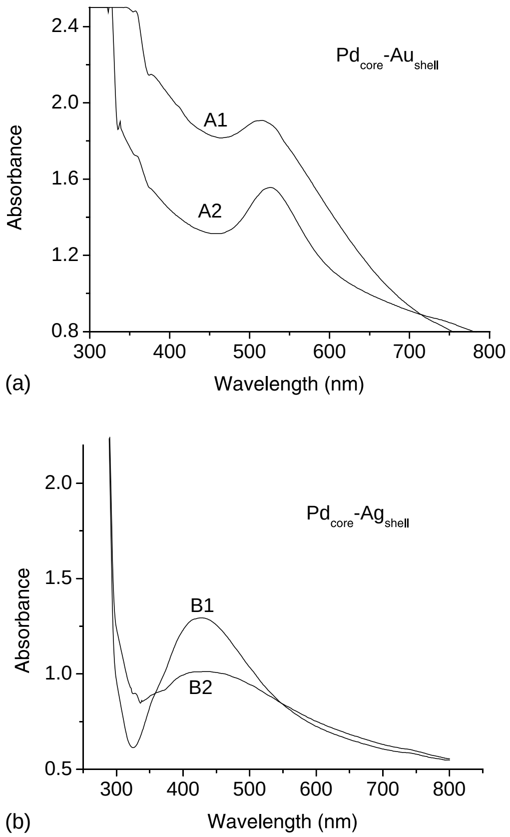

Fig. 2. Plasmon absorption spectrum of (a) Pd_{core}–Au_{shell} (two sets A1 and A2) and (b) Pd_{core}–Ag_{shell} (two sets B1 and B2) particles varying the seed concentration but keeping the Au and Ag ion concentration fixed. Condition for sets A1 [Pd(0)] = 2.2×10^{-4} M and [$HAuCl_4$] = 4.4×10^{-4} M; A2 [Pd(0)] = 1.1×10^{-4} M and [$HAuCl_4$] = 4.4×10^{-4} M; B1 [Pd(0)] = 2.2×10^{-4} M and [$AgNO_3$] = 4.4×10^{-4} M; B2 [Pd(0)] = 1.1×10^{-4} M and [$AgNO_3$] = 4.4×10^{-4} M; [TX-100] = 10^{-2} M for always.

The particles of Pd/Au and Pd/Ag combinations had the Pd_{core}–Au_{shell} and Pd_{core}–Ag_{shell} structures. The starting material was 5.5×10^{-5} M Pd(0) colloid in TX-100. Varying amounts of $HAuCl_4$ solutions were loaded and reduced along with Pd particles by the same photoactivation technique and plasmon absorption band were recorded for different compositions of Pd:Au (Fig. 1). At a molar ratio of 1:0.5 (Pd:Au) bimetallic particles showed no plasmon absorption band corresponding to gold nanoparticles. However, with the ratio of 1:1, a band due to Au(0) appeared with a λ_{max} at 510 nm which indicated new particle formation. With further increasing the Au(III) ion loading the deposition of increased amount of Au(0) was observed and interestingly the λ_{max} of the plasmon band for gold gradually shifted towards the red region (510 nm for 1:1,

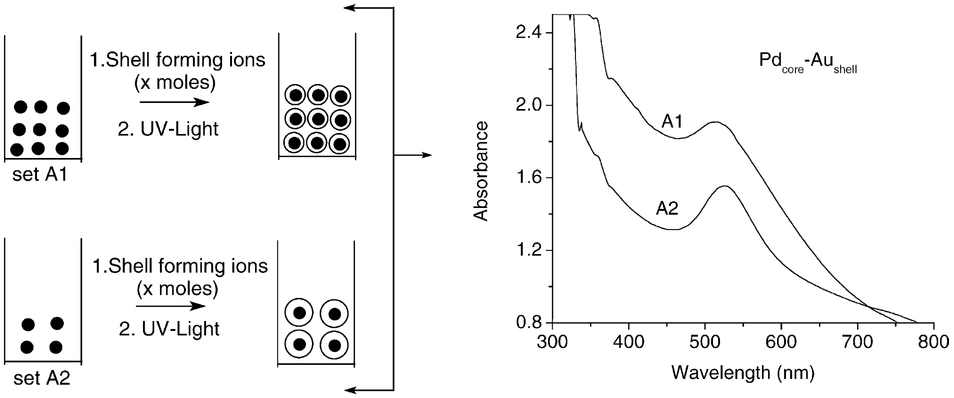

Scheme 1. Schematic presentation of thickening of shell depending upon the population of seed upon addition of fixed amount of shell forming ions.

515 nm for 1:2, 520 nm for 1:3 and 525 nm for 1:4). However, solutions containing mixtures of preformed Pd(0) and Au(0) in TX-100 with similar compositions always showed a peak at ~523 nm comparable to the plasmon absorption band of pure gold particles [43,44]. These characteristic absorption bands were compared with the published literature [38]. Hence the formation of core–shell (Pd_{core}–Au_{shell}) structures due to Pd/Au combinations were authenticated. Similar observation was also noticed (Pd_{core}–Ag_{shell} structures) for Pd/Ag combination while photoactivation was done with Pd seeds and various amounts of $AgNO_3$ in TX-100.

One might argue that Au(0) particles are present independently as separate entity along with Pd(0) particles in a mixture as the colloidal suspension. To substantiate the answer and to authenticate the evolution of core–shell structures we performed experiments varying the seed concentration, i.e. Pd(0) but keeping the Au(III) ion (shell forming ion) concentration fixed. We made two sets (A1, A2) having the composition of Pd:Au = 1:2 ($[Pd(0)] = 2.2 \times 10^{-4}$ M and $[HAuCl_4] = 4.4 \times 10^{-4}$ M) and 1:4 ($[Pd(0)] = 1.1 \times 10^{-4}$ M and $[HAuCl_4] = 4.4 \times 10^{-4}$ M), respectively, and recorded their plasmon absorption bands (Fig. 2(a)) after UV-irradiation. We observed a red shifting of the plasmon

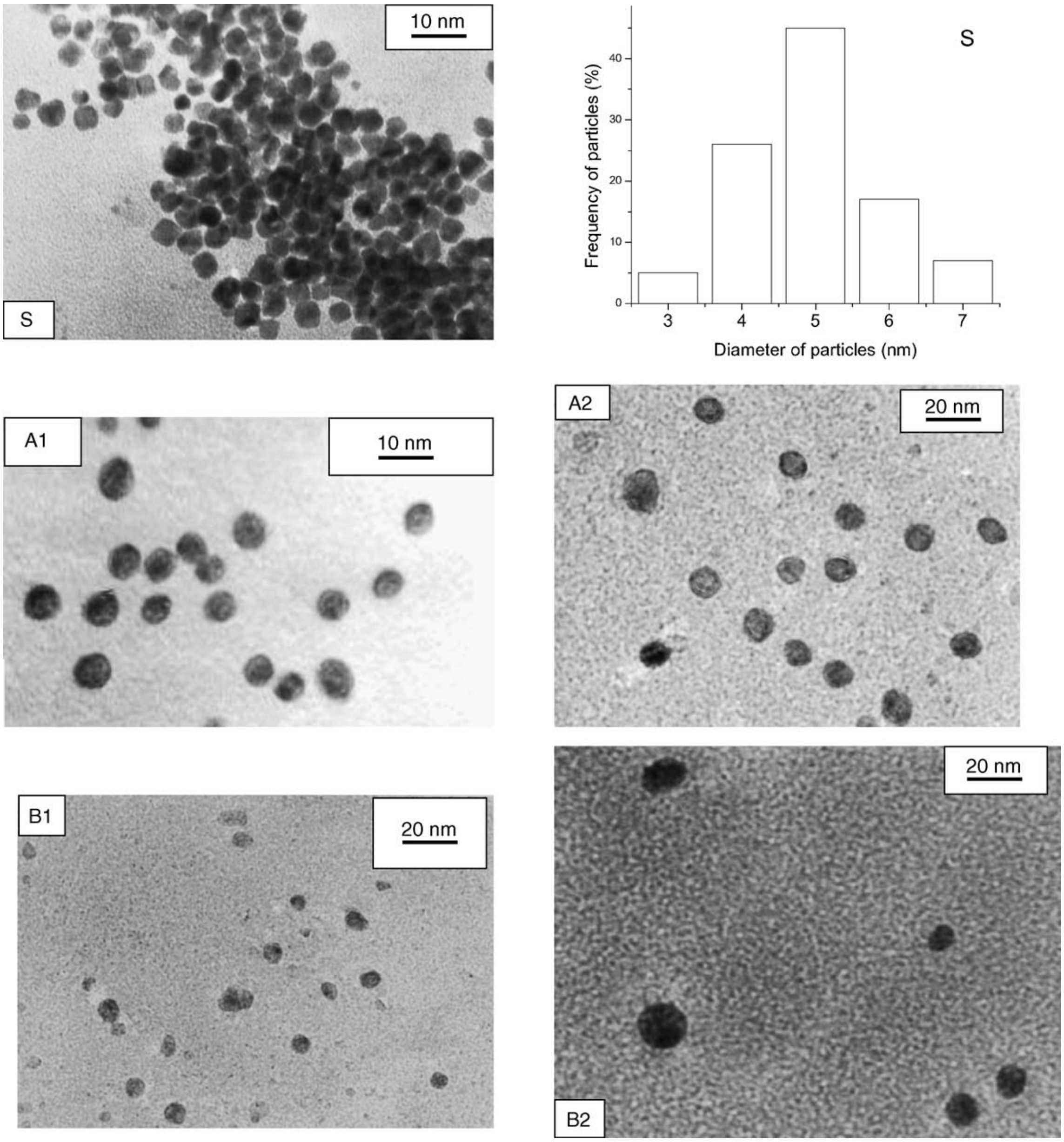

Fig. 3. Transmission electron micrograph (TEM) of seed (S) and different sets of Pd_{core}–Au_{shell} and Pd_{core}–Ag_{shell} nanoparticles (A1, A2, B1, B2). Condition for sets S $[Pd(0)] = 2.2 \times 10^{-4}$ M; A1 $[Pd(0)] = 2.2 \times 10^{-4}$ M and $[HAuCl_4] = 4.4 \times 10^{-4}$ M; A2 $[Pd(0)] = 1.1 \times 10^{-4}$ M and $[HAuCl_4] = 4.4 \times 10^{-4}$ M; B1 $[Pd(0)] = 2.2 \times 10^{-4}$ M and $[AgNO_3] = 4.4 \times 10^{-4}$ M; B2 $[Pd(0)] = 1.1 \times 10^{-4}$ M and $[AgNO_3] = 4.4 \times 10^{-4}$ M; $[TX\text{-}100] = 10^{-2}$ M.

absorption band from 520 to 530 nm as the seed concentration is decreased (A1–A2). This suggests the formation of larger particles (higher shell thickness) owing to the presence of less number of Pd particles in A2 compared to A1. Moreover, the absorbance value of the plasmon band at the λ_{max} for the two sets (A1 and A2) varies with seed concentration (absorbance increases with seed concentration). This suggests relatively smaller population of larger core–shell particles for lower seed concentration. Hence, it is spelt out that optical properties of the core–shell nanoparticle are dominated by Au shell and the plasmon band is red shifted as the Au shell is gradually thickened with the decrease of Pd-seed population for a fixed amount of Au(III) ions (Scheme 1). From this, we can reasonably infer that the reduction of Au-salt occurs on the surface of the preformed Pd particles rather than the formation of new nucleation centers. Similar result was also observed by Wang et al. and Jana et al. in case of the formation of Au_{core}–Ag_{shell} type bimetallic nanoparticles [45,46]. Again for Pd_{core}–Ag_{shell} particle formation, similar phenomenon happened when we carried out the experiment in similar fashion keeping the silver ion concentration fixed but varying the seed concentration. The plasmon absorption band for two sets of Pd_{core}–Ag_{shell} particles taking the ratio of Pd:Ag = 1:2 (set B1 $[Pd(0)] = 2.2 \times 10^{-4}$ M and $[AgNO_3] = 4.4 \times 10^{-4}$ M) and 1:4 (set B2 $[Pd(0)] = 1.1 \times 10^{-4}$ M and $[AgNO_3] = 4.4 \times 10^{-4}$ M) are shown in Fig. 2(b). Here also plasmon absorption band appeared with a λ_{max} at 425 nm for set B1, which is exclusively attributed to Ag-plasmon absorption band indicating wrapping of Pd particles by Ag layers and with the decrease of seed concentration the red shifting of plasmon absorption from 425 to 435 nm was observed (cf. to A1 and A2 cases). This again suggests the formation of larger particles with the decrease in seed concentration due to deposition of higher amount of Ag onto the less number of Pd seeds. It should be borne in mind that smaller seed concentration implies lower population of particles. Subsequent addition of adlayers (shells) onto the particles would readily increase the size of the bimetallics. Therefore, a solution with lower number of seed particles would enhance the size of the particles in comparison to those of solution containing higher number of seed particles for addition of same amount of shell forming metal ions. The TEM images of seed (S) and different core–shell particles of Pd/Au (A1 and A2) and Pd/Ag (B1 and B2) are displayed in Fig. 3. From the TEM images it is observed that the particles are almost monodisperse with spherical shapes. The pure Pd particles have a strong tendency to form cluster, this tendency became less pronounced for the gold and silver covered particles. From the TEM images it is evident that the core–shell type bimetallic particles are larger in size than the seed particles and size of the particles increases as the seed concentration decreases. For the less populated seed solution higher amounts of the Au(III) ion was adsorbed onto the seed particles and after getting reduced a thicker shell was formed and hence, the size of the core–shell particles became larger and plasmon absorption band shifted to red region as authenticated by others. Under the experimental condition (30 min irradiation), complete reduction of the added metal ions (Au and Ag) was confirmed from the ICP studies taking the supernatant solution of the exposed solutions. The EDX measurements were carried out by illuminating the electron beam on a selected particle of interest. When an electron beam was sharpened and aimed at the edge of the bimetallic particles, where the contrast of the image was weaker than that at the center, the edge was found to consist of gold. When the whole part of the particle was exposed to a broadened electron beam, the obtained Pd:Au ratio were approximately consistent with Pd(II):Au(III). The results are shown in Table 1. The EDX results clearly show that the bimetallic nanoparticles are composed of palladium core and gold shell. The EDX pattern indicates the polycrystalline nature of the particles rather than single crystalline nature. One of the representatives EDX pattern for Pd_{core}–Au_{shell} structure is shown in Fig. 4.

Table 1
Atomic composition of Pd and Au at edge and center of three different particles of set A1

Element	Atomic percentage at edge			Atomic percentage at center		
Au	93.69	92.07	91.76	66.88	64.65	68.51
Pd	6.31	7.93	8.24	33.12	35.35	31.49

Fig. 4. Electron dispersive X-ray (EDX) pattern of Pd_{core}–Au_{shell} particles for set A1.

4. Plausible mechanism

The seed particles of Pd(0) were generated by UV-photoactivation technique. Later individually the Au or Ag salt was added to seed solution of Pd(0) taken in TX-100. The ions of gold and silver are adsorbed on the seed particles and those ions in turn get reduced to the corresponding metal resulting out the core–shell particles of Pd/Au or Pd/Ag by UV-photoactivation technique. So enlargement of particles occurs. Here, the TX-100 molecules were exploited as reducing agent as well as stabilizer. The TX-100 molecules $[R–OCH_2CH_2–OH]$ where $[R = (CH_3)_3\ C\ CH_2C(CH_3)_2\ C_6H_4(OCH_2CH_2)_{\sim 9}{}^{-}]$ having the '–OH' group help to reduce the Pd(II) to Pd(0), Au(III) to Au(0) and Ag(I) to Ag(0). At first, there is an efficient absorption of UV-light by aqueous solution of $PdCl_2$. The $PdCl_2$ then transfers the energy to the TX-100 molecules under consideration. The alcoholic functionality of TX-100 molecules reduces Pd(II) species to Pd(0) and in turn, the terminal '$–CH_2OH$' functionality is oxidized to carboxyl (–COOH) group which has been characterized from IR spectra [44].

5. Conclusion

The novelty of this seed-mediated method lies in its simplicity and control over the size for particle evolution only by varying the seed to shell forming ion concentrations without the use of any new capping agent or template. The technique does not increase the local concentration of the reducing agent in any stage. The seed-mediated technique or its modified version may be useful model for other systems of nanoparticles to produce the particles of desired size without the need of any skill hand or whatever.

Acknowledgements

Authors are grateful to CSIR and DST, New Delhi, for financial assistance.

References

[1] H.D. Robert, P. Rao, J. Mater. Res. 11 (1996) 2834.
[2] S. Link, M.A. El-Sayed, J. Phys. Chem. B 103 (1999) 8410.
[3] L. Polato, L.M. Benedetti, L. Callegaro, J. Drug Target. 2 (1994) 53.
[4] N. Pradhan, A. Pal, T. Pal, Langmuir 17 (2001) 1800.
[5] N.R. Jana, T. Pal, Langmuir 15 (1999) 3458.
[6] N.R. Jana, T.K. Sau, T. Pal, J. Phys. Chem. B 103 (1999) 115.
[7] N. Cordente, M. Respaud, F. Senocq, M.J. Casanove, C. Amiens, B. Chaudret, Nanoletters 1 (2001) 565.
[8] M. Tanase, L.A. Bauer, A. Hultgren, D.M. Silevitch, L. Sun, D.H. Reich, P.C. Searson, G.J. Meyer, Nanoletters 1 (2001) 155.
[9] N. Toshima, T. Yonezawa, N. J. Chem. 11 (1998) 1179.
[10] R.W.J. Scott, A.K. Datye, R.M. Crooks, J. Am. Chem. Soc. 125 (2003) 3708.
[11] N. Toshima, M. Harada, Y. Yamazaki, K. Asakura, J. Phys. Chem. 96 (1992) 9927.
[12] S.W. Han, Y. Kim, K. Kim, J. Colloid Interf. Sci. 208 (1998) 272.
[13] N. Toshima, T. Yonezawa, K. Kushihashi, J. Chem. Soc., Faraday Trans. 89 (1993) 2537.
[14] N. Toshima, Y. Wang, Langmuir 10 (1994) 4574.
[15] T. Yonezawa, N. Toshima, J. Chem. Soc., Faraday Trans. 91 (1995) 4111.
[16] S. Link, Z.L. Wang, M.A. El-Sayed, J. Phys. Chem. B 103 (1999) 3529.
[17] N. Toshima, P. Lu, Chem. Lett. (1996) 729.
[18] P.-Y. Silvert, V. Vijayakrishnan, P. Vibert, R. Herrera-Urbina, K.T. Elhsissen, Nanostruct. Mater. 7 (1996) 611.
[19] Y. Mizukoshi, K. Okitsu, Y. Maeda, T.A. Yamamoto, R. Oshima, Y. Nagata, J. Phys. Chem. B 101 (1997) 7033.
[20] S. Remita, M. Mostafavi, M.O. Delcourt, Radiat. Phys. Chem. 47 (1996) 275.
[21] J.H. Hodak, A. Henglein, M. Giersig, G.V. Hartland, J. Phys. Chem. B 104 (2000) 11708.
[22] Y.H. Chen, C.S. Yeh, Chem. Commun. (2000) 371.
[23] M. Treguer, C. de Cointet, H. Remita, J. Khatouri, M. Mostafavi, J. Amblard, J. Belloni, R. de Keyzer, J. Phys. Chem. B 102 (1998) 4310.
[24] M. Mandal, S. Kundu, S.K. Ghosh, T.K. Sau, S.M. Yusuf, T. Pal, J. Colloid Interf. Sci. 265 (2003) 23.
[25] K. Mallik, M. Mandal, N. Pradhan, T. Pal, Nanoletters 1 (2001) 319.
[26] (a) S. Schauermann, J. Hoffmann, V. Johanek, J. Hartmann, J. Libuda, H.-J. Freund, Catal. Lett. 84 (2002) 209;
(b) R. Narayanan, M.A. El-Sayed, J. Am. Chem. Soc. 125 (2003) 8340.
[27] A.F. Lee, C.J. Baddeley, C. Hardacre, R.M. Ormerod, R.C. Lambert, G. Schmid, H. West, J. Phys. Chem. 99 (1995) 6096.
[28] Y. Mizukoshi, T. Fujimoto, Y. Nagata, R. Oshima, Y. Mayeda, J. Phys. Chem. B 104 (2000) 6028.
[29] H.N. Vasan, C.N.R. Rao, J. Mater. Chem. 5 (1995) 1755.
[30] C.Y. Huang, H.J. Chiang, J.C. Huang, S.R. Sheen, Nanostruct. Mater. 10 (1998) 1393.
[31] K. Esumi, M. Wakabayashi, K. Torigoe, Colloid Surf. A 109 (1996) 55.
[32] H. Remita, J.K. Khatouri, M. Treguer, J. Amblard, J. Belloni, Z. Phys. D 40 (1997) 127.
[33] M.-L. Wu, D.-H. Chen, T.-C. Huang, Langmuir 17 (2001) 3877.
[34] H. Liu, G. Mao, M. Meng, J. Mol. Catal. 74 (1992) 6028.
[35] G. Schmid, A. Lehnert, J.-O. Malm, J.-O. Bovin, Angew. Chem. Int. Ed. Engl. 30 (1991) 874.
[36] R. Oshima, T.A. Yamamoto, Y. Mizukosi, Y. Nagata, Y. Maeda, Nanostruct. Mater. 12 (1999) 111.
[37] K. Okitsu, M. Murakami, S. Tanabe, H. Matsumoto, Chem. Lett. (2000) 1336.
[38] A. Henglein, J. Phys. Chem. B 104 (2000) 6683.
[39] M. Zhao, R.M. Crooks, Angew. Chem. Int. Ed. 38 (1999) 364.
[40] M. Mandal, S.K. Ghosh, S. Kundu, K. Esumi, T. Pal, Langmuir 18 (2002) 7792.
[41] S.K. Ghosh, S. Kundu, M. Mandal, S. Nath, T. Pal, J. Nanopart. Res. 5 (2003) 577.
[42] T.K. Sau, A. Pal, N.R. Jana, Z.L. Wang, T. Pal, J. Nanopart. Res. 3 (2001) 257.
[43] A. Henglein, Langmuir 15 (1999) 6738.
[44] A. Pal, Talanta 46 (1998) 583.
[45] L. Lu, H. Wang, Y. Zhou, S. Xi, H. Zhang, J. Hu, B. Zhao, Chem. Commun. (2002) 144.
[46] N.R. Jana, L. Gearheart, C.J. Murphy, Chem. Mater. 13 (2001) 2313.